Potential inhibiting activities of phytochemicals in *Scilla natalensis* bulbs against schistosomiasis

Abel Kolawole Oyebamiji[1+], Jonathan Oyebamiji Babalola[2], Kehinde Abraham Odelade[3], Sunday Adewale Akintelu[4], Olubunmi Ayoola Nubi[5], Halleluyah Oluwatobi Aworinde[6], Esther Faboro[1], Emmanuel Temitope Akintayo[1], Banjo Semire[7]

1. Bowen University, Department of Chemistry and Industrial Chemistry, Iwo, Nigeria.
2. University of Ibadan, Department of Chemistry, Ibadan, Nigeria.
3. Federal Polytechnic, Department of Science Laboratory Technology, Ayede, Nigeria.
4. Beijing Institute of Technology, School of Chemistry and Chemical Engineering, Beijing, China.
5. Nigerian Institute for Oceanography & Marine Research, Victoria Island, Nigeria.
6. Bowen University, College of Computing and Communication Studies, Iwo, Nigeria.
7. Ladoke Akintola University of Technology, Department of Pure and Applied Chemistry, Ogbomoso, Nigeria.

+Corresponding author: Abel Kolawole Oyebamiji, **Phone:** +2348032493676, **Email address:** abeloyebamiji@gmail.com

ABSTRACT: Schistosomiasis remains one of the severe ailments that affect both man and woman in South Africa. It is caused by blood fluke, and the rate at which it causes death is alarming in some areas of America, Asia as well as in African countries. It is a neglected tropical disease (NTD) with grave impact on social and economic situation of countries with low sanitation awareness. Thus, the search for lasting solution to this menace, has drawn the attention of many global researchers using phytochemicals from *Scilla natalensis* via *in silico* approach. The studied compounds were optimized using Spartan 14. Docking study was executed via Pymol, Autodock tool, Auto dock vina and discovery studio. Compound **9** with –34.3 kJ mol^{-1} and –39.3 kJ mol^{-1} as binding affinity proved to possess highest ability to inhibit glutathione S-transferase and thioredoxin-glutathione reductase than other compounds. Also, ADMET properties for compound **9** and praziquantel were explored and reported. Our findings may open the door for the design of novel drug-like molecules with better
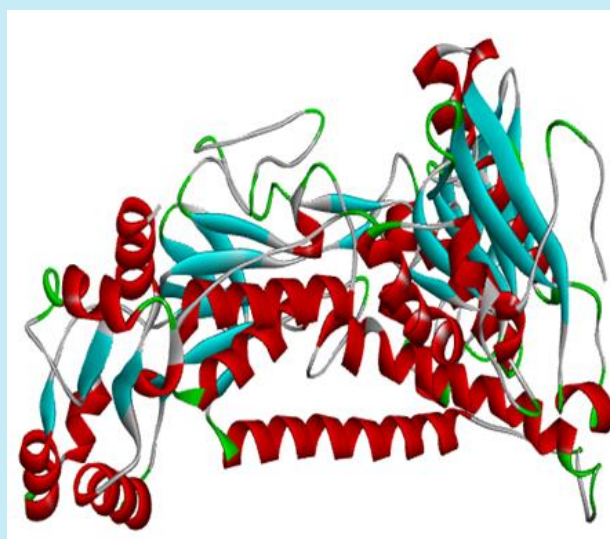
1. Introduction

Neglected tropical diseases (NTDs) are a class of syndromes that occur in tropical and subtropical regions most especially in developing countries (Engels and Zhou, 2020). The continuous spreading and the lingering effects of these types of diseases have been acknowledged to be a function of poverty. According to Ugbe *et al.* (2022), improper treatment of sickness and frequent lack of access to pure water are some of the variables that increase the prevalence of NTDs in local settlements. Series of reports about greater effort to curb diseases, like malaria, tuberculosis, etc., from national and international agencies show that NTDs are completely neglected diseases (Allotey *et al.*, 2010; Molyneux, 2008; 2009). Some of the NTDs are schistosomiasis, Buruli ulcer, trachoma, dengue virus, Guinea worm disease and onchocerciasis (WHO, 2022). The cost of treating NTDs is relatively small in some instances; however, due to poverty or low income, some areas in Africa, America and Asia are still experiencing greatly the effects of NTDs (Reddy *et al.*, 2007).

However, grave operation of schistosomiasis in human has drawn the attention of the World Health Organization (WHO), and it has been categorized as part of the 20 considered NTDs (Colley *et al.*, 2014; WHO, 2020). The name of this disease originated from *Schistosoma*, to which the worm (trematode) that causes it belongs. The taxonomic order of *Schistosoma* is kingdom: Animalia; phylum: Platyhelminthes; order: Diplostomida; subfamilly: Schistosomatinae; genus: *Schitosoma* and species: *haematobium, mansoni, japonicum*, *guineensis*, *intercalatum*, and *mekongi* (Kayuni *et al.*, 2019). Some of these species are the most common disease-causing species, while the remaining ones have lower universal pervasiveness. According to Klohe *et al.* (2021), the effects of schistosomiasis have been recorded in over 70 countries of which over 80% possess moderate to high spread, which requires serious mediation via precautionary chemotherapy. As reported by Porto *et al.* (2021), more than 2 million people have been affected while 800 million people were reported to be at risk of this deadly disease. Despite various efforts to contain this menace, its deadly operation in tropical and subtropical regions requires urgent and rapid intervention by means of potent chemotherapeutic agents.

Scilla natalensis is a bulbous herb with many medicinal features. It is a plant with blue flowers, and it is regarded as one of the well-known plant species with high demand in the South African market (Sparg *et al.*, 2002). As reported by several scientists, *S. natalensis* has been used to treat a series of diseases and infections, such as worms, stomach aches, fractures, boils, veld sores, skin rashes, diarrhea, constipation, dysentery, nausea, and indigestion (Cunningham, 1988; Eloff, 1998; Mander, 1997). Its bulb has the ability to act as laxative for tumors within the body and lumps, male potency enhancer and woman fertility booster. It subdues pain that originated from menstruation, and it eases child delivery for pregnant women (Hutchings, 1989; Hutchings *et al.*, 1996). The extract from *S. natalensis* was screened for anti-inflammatory and anthelmintic activity, and the results showed that the hexane extracts of *S. natalensis* displayed good inhibition against both COX-1 and COX-2 (Sparg *et al.*, 2002).
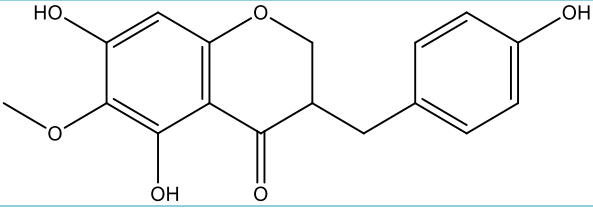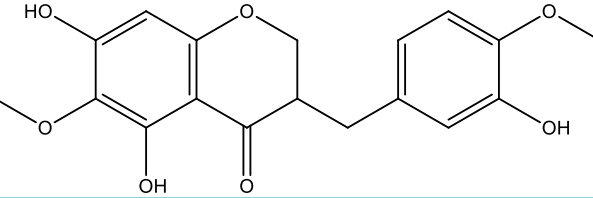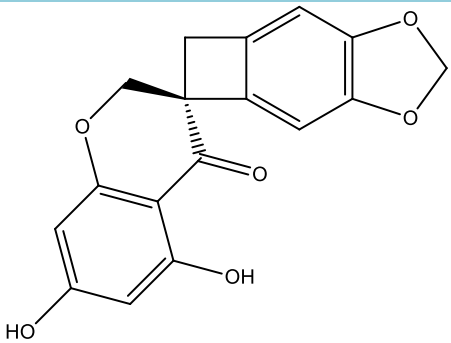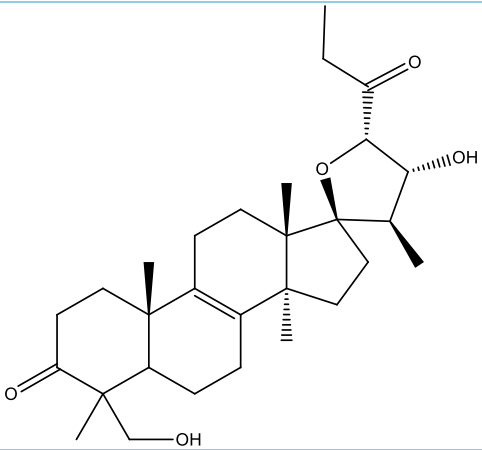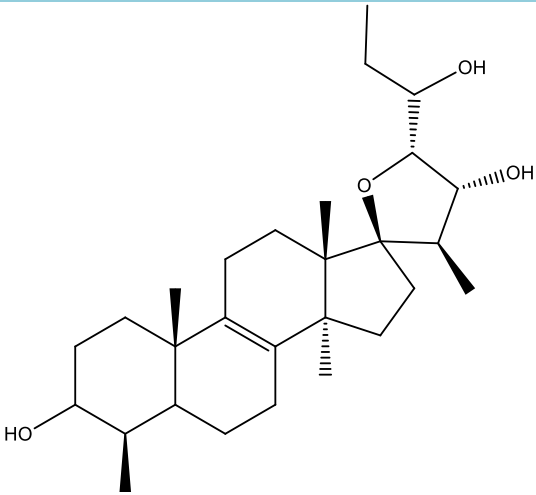
Therefore, the main purpose of this work is to (i) explore theoretical biological features of the selected phytochemicals obtained from *S. natalensis,* (ii) investigate the calculated binding affinity between the selected phytochemicals and the targets, and (iii) theoretically explore the pharmacokinetics of the selected phytochemicals.

2. Materials and methods

2.1 Structural optimization

The selected compounds from *S. natalensis* bulb were carefully modeled using ChemDraw Ultra 12.0.2 software and saved as MDL SDfile (*.sdf) format (Table 1). The modeled structures were subjected to Spartan'14 software to view a 3D version of the modeled structures and then optimized via energy minimization. The minimization of the studied molecular compounds was executed using Molecular Mechanics Force Field, while the optimization of the compounds was accomplished using density functional theory (DFT) and 6-31G* was used as basis set. The optimized compounds were saved and the calculated descriptors for each molecule were reported (Oyeneyin *et al.*, 2022; Wang *et al.*, 2020).

Table 1. Two-dimensional (2D) structure of the studied compound.

	Chemical structure	IUPAC names
1		5,7-dihydroxy-6-methoxy-3-(4-hydroxybenzyl)chroman-4-one
2		5,7-dihydroxy-6-methoxy-3-(3-hydroxy-4-methoxybenzyl)chroman-4-one
3		(3*R*)-5,7-dihydroxyspiro[2*H*-chromene-3,4'-9,11-dioxatricyclo[6.3.0.0^{3,6}]undeca-1(8),2,6-triene]-4-one
4		(22*R*,23*S*)-17α,23-Epoxy-22,29-dihydroxy-27-norlanost-8-en-3,24-dione
5		(22*R*,23*S*)-17α,23-Epoxy-3β,22,24ξ-trihydroxy-27,28-bisnor-lanost-8-ene
		Continue…

6		(23*S*)-17α,23-Epoxy-3β,24ξ-dihydroxy-27,28,29-trisnorlanost-8-ene
7		5,7 -dihydroxy-3-(3hydroxy-4-methoxybenzyl)chroman-4-one
8		5-[(3*S*,8*R*,9*S*,10*R*,13*R*,14*S*,17*R*)-3-[(2*R*,3*R*,4*S*,5*R*,6*S*)-3,4-dihydroxy-6-methyl-5-[(2*S*,3*R*,4*S*,5*S*,6*R*)-3,4,5-trihydroxy-6-(hydroxymethyl)oxan-2-yl]oxyoxan-2-yl]oxy-14-hydroxy-10,13-dimethyl-1,2,3,6,7,8,9,11,12,15,16,17-dodecahydrocyclopenta[a]phenanthren-17-yl]pyran-2-one
9		5-[(3*S*,8*R*,9*S*,10*R*,13*R*,14*S*,17*R*)-14-hydroxy-10,13-dimethyl-3-(3,4,5-trihydroxy-6-methyloxan-2-yl)oxy-1,2,3,6,7,8,9,11,12,15,16,17-dodecahydrocyclopenta[a]phenanthren-17-yl]pyran-2-one
10		5-[(3*S*,8*R*,9*S*,10*R*,13*R*,14*S*,17*R*)-3,14-dihydroxy-10,13-dimethyl-1,2,3,6,7,8,9,11,12,15,16,17-dodecahydrocyclopenta[a]phenanthren-17-yl]pyran-2-one
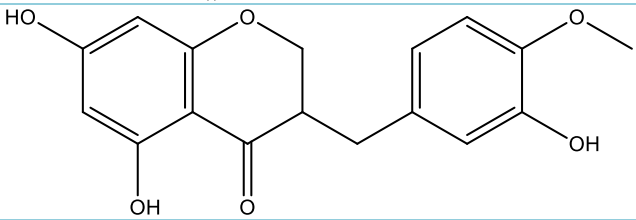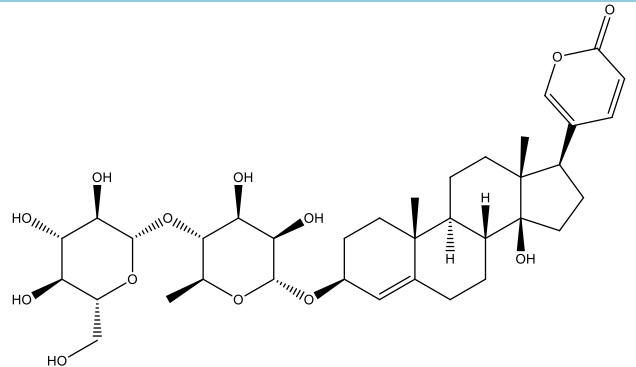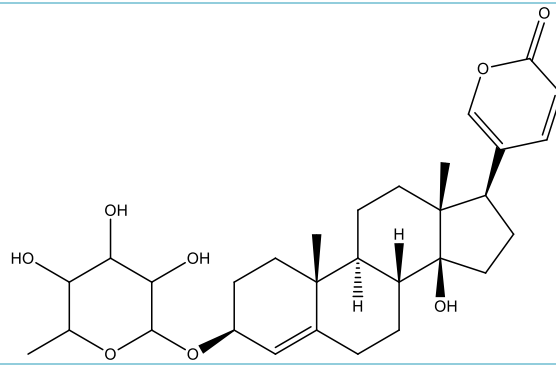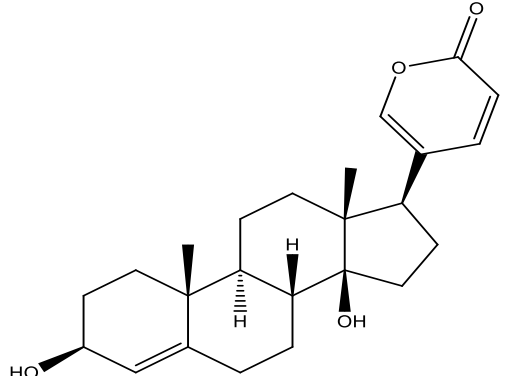
Source: Elaborated by the authors using data from Sparg *et al.*, (2002).

2.2 Target identification, selection and preparation

Two targets (glutathione S-transferase [PDB ID: 1gtb]) (McTigue *et al.*, 1995) and thioredoxin-glutathione reductase (PDB ID: 3h4k) (Angelucci *et al.*, 2009) were retrieved from protein data bank (Fig. 1a and b). The two receptors were subjected to Pymol software where suitable implements were deployed to treat and prepare glutathione S-transferase (PDB ID: 1gtb) and thioredoxin-glutathione reductase (PDB ID: 3h4k) for docking. The amino acids present in each of the downloaded receptor were carefully checked and any other materials (i.e., crystallographic water and small molecules rooted in each of the receptor) different from amino acids were deleted and saved in *.pdb format.

Also, all the possible missing amino acids in each clean receptor were replaced using Swiss Pdbviewer 4.1.0 version and saved in *.pdb format before identification of the binding site in each receptor using Autodock tool software. The center and size in X, Y and Z directions which show the located binding site for glutathione S-transferase (PDB ID: 1gtb) were 11.97, 45.043 and 32.999 for the center and 50, 52 and 60 for size; and for thioredoxin-glutathione reductase (PDB ID: 3h4k) were 45.78, –0.593 and 16.04 for the center and 80, 90 and 78 for size. The calculation of binding affinity for the studied complex was executed via Autodock vina software and the discovery studio was used to view the interaction between the ligands and the receptors.
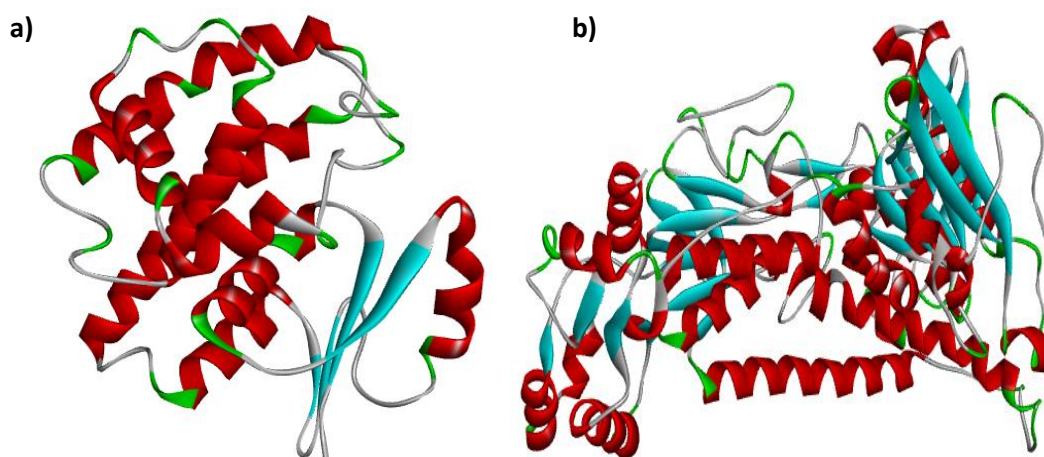

Figure 1. Tree-dimensional (3D) structures of transferase and reductase enzymes: (**a**) 3D structure of glutathione S-transferase and (**b**) 3D structure of thioredoxin-glutathione reductase.

2.3 Computational analysis of pharmacokinetic properties

The study of pharmacokinetics plays a crucial role in drug design and discovery since only chemical compounds with worthy drug-likeness features, as well as outstanding absorption, distribution, metabolism, excretion, and toxicity (ADMET) profiles move into the advance stage of drug production (Lawal *et al.*, 2021). Therefore, 5-[(3*S*,8*R*,9*S*,10*R*,13*R*,14*S*,17*R*)-14-hydroxy-10,13-dimethyl-3-(3,4,5-trihydroxy-6-methyloxan-2-yl)oxy-1,2,3,6,7,8,9,11,12,15,16,17-dodecahydrocyclopenta[a]phenanthren-17-yl]pyran-2-one (**9**) with lower binding affinity value, which indicate better inhibitory activities, was reconnoitered for ADMET study via ADMETlab (https://admetmesh.scbdd.com/), an online ADMET software.

3. Results and discussion

3.1 Calculated descriptors

One of the crucial descriptors calculated from optimized molecular compounds as described by many researchers are the highest occupied molecular orbital energy (E_{HOMO}), and lowest unoccupied molecular orbital energy (E_{LUMO}) (HOMO-LUMO energies). The part taken in overriding vast array of chemical and biological interactions by HOMO-LUMO energies cannot be easily neglected (Saranya *et al.*, 2018). The E_{HOMO} indicates molecule with greater strength to donate electron while E_{LUMO} indicate molecules with greater strength to accept electron from neighboring compounds. In this work, we observed that (3*R*)-5,7-dihydroxyspiro[2*H*-chromene-3,4'-9,11-dioxatricyclo[6.3.0.0^{3,6}]undeca-1(8),2,6-triene]-4-one (**3**) has highest strength to donate and receive electrons

from nearby compounds. Also, lower band gap indicates spontaneous interactions between two molecules (Latona *et al.* 2022a); thus, (3*R*)-5,7-dihydroxyspiro[2*H*-chromene-3,4'9,11-dioxatricyclo[6.3.0.0³,⁶]undeca-1(8),2,6-triene]-4-one (**3**) showed a greater strength to interact with neighboring compounds than other studied compounds (Supplementary Material 1). As we observed in this work, lower number of atoms highly contributed

to high level of interacting ability of compound **3**; this revealed the effectiveness of the combination of the atom as well as the bonds present in (3*R*)-5,7-dihydroxyspiro[2*H*-chromene-3,4'-9,11-dioxatricyclo[6.3.0.0³,⁶]undeca-1(8),2,6-triene]-4-one (**3**). Other descriptors obtained from compounds from *S. natalensis* bulb were also reported in Table 2.

Table 2. The selected descriptors obtained from compounds from *S. natalensis* bulb.

	E$_{HOMO}$	E$_{LUMO}$	BG	MW	LogP	HBD	HBA
1	−5.76	−1.48	4.28	316.30	−2.66	3.00	6.00
2	−5.59	−1.49	4.10	346.33	−3.64	3.00	7.00
3	−5.58	−1.61	3.97	312.27	−2.97	2.00	6.00
4	−5.77	−0.97	4.80	472.66	4.62	2.00	5.00
5	−5.79	0.82	6.61	446.67	4.34	3.00	4.00
6	−5.80	0.80	6.60	416.64	4.76	2.00	3.00
7	−5.59	−1.44	4.15	316.30	−2.66	3.00	6.00
8	−6.25	−1.36	4.89	692.79	0.73	7.00	12.00
9	−6.28	−1.44	4.84	530.65	2.47	4.00	7.00
10	−6.28	−1.44	4.84	384.51	3.36	2.00	3.00

3.2 Molecular docking analysis

The assessment of the orientation of the selected compounds from *S. natalensis* bulb in the active site of the targets glutathione S-transferase (PDB ID: 1gtb) and thioredoxin-glutathione reductase (PDB ID: 3h4k) were carefully studied using docking method. The biochemical and biological connections between the studied complexes were exposed as well as the calculated binding affinity for the studied complexes were thoroughly investigated and reported. Adeoye *et al.* (2022) reported that biochemical and biological capability of any compound may and may not reveal its inhibition capacity. The inhibition capacity of any compound against the target is a function of the type of nonbonding interactions that occur between such complexes (Latona *et al.*, 2022b). Therefore, 5-[(3*S*,8*R*,9*S*,10*R*,13*R*,14*S*,17*R*)-14-hydroxy-10,13-dimethyl-3-(3,4,5-trihydroxy-6-methyloxan-2-yl)oxy-1,2,3,6,7,8,9,11,12,15,16,17-dodecahydrocyclopenta[a]phenanthren-17-yl]pyran-2-one (compound **9**) with −34.3 kJ mol⁻¹ (PDB ID: 1gtb) and −39.3 kJ mol⁻¹ (PDB ID: 3h4k) possessed greater tendency to inhibit glutathione S-transferase and thioredoxin-glutathione reductase than other studied compounds (Figs. 2 and 3). The calculated binding affinities for compound **1–10** against glutathione S-transferase (PDB ID: 1gtb) were −29.7, −29.3, −31.0, −31.4, −31.8, −33.5, −30.5, −34.3, −34.3, and −31.4 kJ mol⁻¹, respectively. This showed that all the compounds, except compounds 1, 2 and 7, could be good

inhibitors for glutathione S-transferase as compared to Praziquantel. Also, docking results of optimized compounds **1–10** against thioredoxin-glutathione reductase (PDB ID: 3h4k) were −31.8, −32.2, −34.3, −33.9, −34.3, −33.5, −32.6, −34.7, −39.3, and −36.8 kJ mol⁻¹, respectively, indicating that all the phytochemicals could serve as inhibitors for thioredoxin-glutathione reductase (Table 3). According to Olasupo *et al.* (2021), the lower the binding affinity value of a compound, the better the ability of the compound to inhibit the target; hence, compound **9** has outstanding binding affinity and a greater tendency to inhibit glutathione S-transferase and thioredoxin-glutathione reductase, thereby hindering the activities of schistosomiasis. Also, this work agreed well with the work carried out by El-Seedi *et al.* (2012), which authenticated the biological activity of Asparagaceae as antischistosomiasis. Similar results were reported by Akachukwu *et al.*, (2017) when 27 bioactive compounds of some medicinal plants were screened against *Schistosoma* cell lines (PDB ID: 1M9A and 2X99). The docking results revealed that quercetin-(3`-O 4```)-3``-O-methyl kaempferol and quercetin presented binding energies of −39.41 and −38.99 kJ mol⁻¹ against 1M9A cell lines of *Schistosoma*, respectively. Also, the binding affinities calculated for β-solamarine, solamargine and quercetin-(3`-O 4```)-3``-O-methyl kaempferol against 2X99 cell lines of *Schistosoma* were −38.99, −38.58 and −39.41 kJ mol⁻¹, respectively (Akachukwu *et al.*, 2017). This was similar to binding energy calculated for 5-[(3*S*,8*R*,9*S*,10*R*,13*R*,14*S*,17*R*)-14-hydroxy-10,13-

dimethyl-3-(3,4,5-trihydroxy-6-methyloxan-2-yl)oxy-1,2,3,6,7,8,9,11,12,15,16,17-dodecahydrocyclopenta[a]phenanthren-17-yl]pyran-2-one (9) against thioredoxin-glutathione reductase (PDB ID: 3H4K). This was higher than binding affinities reported by Mtemeli *et al.* (2022) from docking *Cucurbita maxima* against *Schistosoma mansoni* purine nucleoside phosphorylase (*Sm*PNP) and *Schistosoma haematobium* 28-kDa glutathione S-transferase (*Sh*28kDaGST). The results showed that binding affinities of the most promising compounds, momordicoside I aglycone and balsaminoside B were –33.1 and –32.2 kJ mol^{-1} with *Sm*PNP and *Sh*28kDaGST, respectively.
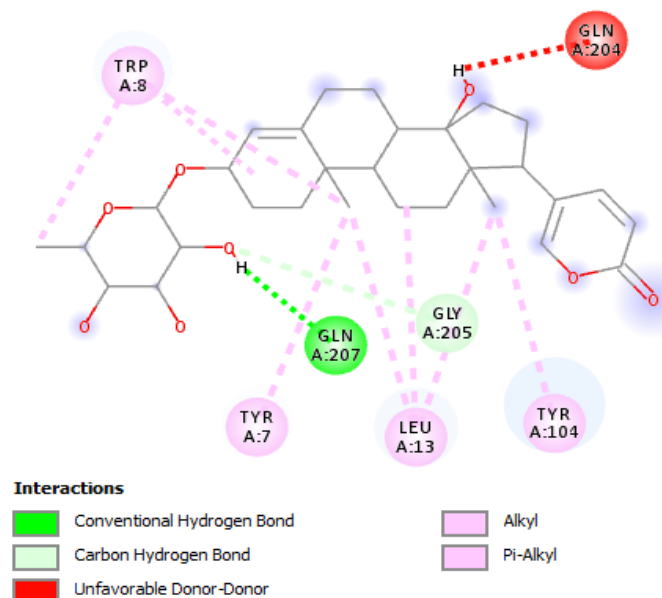

Figure 2. Biochemical interaction between Compound **9** and glutathione S-transferase.
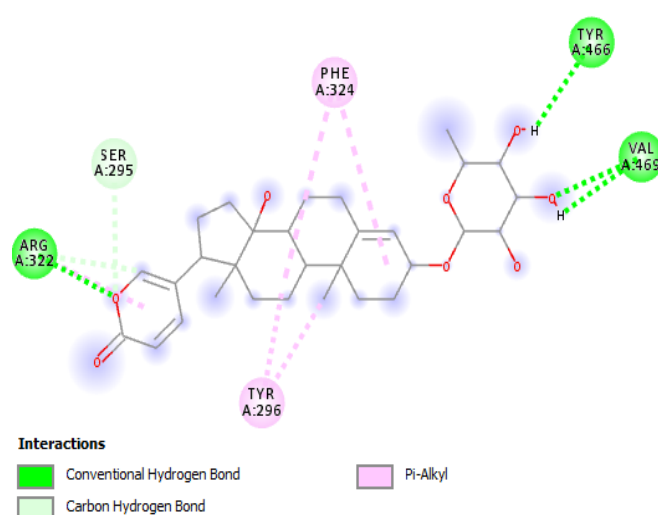
Figure 3. Biochemical interaction between Compound **9** and thioredoxin-glutathione reductase.

Table 3. Calculated binding affinity and residues involved in the interactions.

	Binding affinity (kJ mol^{-1})	
	Glutathione S-transferase	Thioredoxin-glutathione reductase
1	–29.7	–31.8
2	–29.3	–32.2
3	–31.0	–34.3
4	–31.4	–33.9
5	–31.8	–34.3
6	–33.5	–34.7
7	–30.5	–32.6
8	–31.8	–34.7
9	–34.3	–39.3
10	–31.4	–36.8
Praziquantel	–30.1	–33.1

Moreover, the work carried out by El-Seedi *et al.* (2012) on *Asparagus stipularis* Forssk., which was commonly known in Egypt as *agool gabal*, revealed the efficacy of medicinal plant as antischistosomiasis. The extracted asparagalin A was observed to be effective against schistosomiasis. This was confirmed through the efficiency of the studied compound (asparagalin A) against worm egg-laying capacity of *S. mansoni* thereby

down-regulating the activity of schistosomiasis (El-Seedi *et al.*, 2012) and this correlated with the inhibiting activity of the studied *S. natalensis* bulbs.

More so, the inhibiting capacity of three medicinal plants (*Artemisia annua*, *Nigella sativa*, and *Allium sativum*) explored by Fadladdin *et al.* (2022) against *S. mansoni* adult worms was experimentally studied. The concentration of 500 m/dm^3, 250 m/dm^3, and 125 m/dm^3

of *A. annua* proved to be more effective against adult worms when compared to similar concentration of *N. sativa*, and *A. sativum* against the adult worms. Greater morphological changes were observed in the activity of *A. annua* on *S. mansoni* adult worms; however, lesser morphological changes were shown in the activities of *N. sativa*, and *A. sativum* on the *S. mansoni* adult worms. This inhibiting activity of *A. annua* on *S. mansoni* agreed with efficiency of *S. natalensis* bulbs as antischistosomiasis due to greater ability to hinder the activity of *S. mansoni* than praziquantel (reference drug) (Fadladdin *et al.*, 2022).

3.3 Pharmacokinetic study

The ADMET properties for compounds **9** and praziquantel (referenced drug) were accomplished using ADMETlab software and series of factors were considered such as physicochemical property, medicinal chemistry, absorption, distribution, metabolism, excretion, toxicity, environmental toxicity, tox21 pathway, toxicophore rules. The calculated molecular weight for compound **9** fell within the acceptable range of 100–600 amu and this was confirmed to help it physicochemical property. Also, number of hydrogen bond acceptors (0–12), number of hydrogen bond donors (0–7), number of rotatable bonds (0–11), number of rings (0–6), number of atoms in the biggest ring (0–18), number of heteroatoms (1–15), formal charge (–4 to 4), topological polar surface area (0–140) for compound **9** were within the acceptable range and its ability to act as potential drug proved to be valid (Supplementary Material 2 and 3).

As shown in Supplementary Material 2 and 3, synthetic accessibility score (SAscore) for compound **9** (5.052) was within the acceptable range for ease of synthesis of drug-like molecules (< 6) and this showed that compound **9** can easily be synthesized. Also, compound **9** obeyed Lipinski rule of five and other factors considered were reported in Supplementary Material 2 and 3. More so, the ADMET properties for compound **9** were in line with the ADMET properties obtained for the referenced drug (praziquantel).

4. Conclusions

The biochemical and biological activities of selected compounds from *S. natalensis* bulb were thoroughly investigated via *in silico* approach. We observed that *S. natalensis* bulb have the potential anti-schistosomiasis

activities which was described via the calculated descriptors. Also, 5-[(3*S*,8*R*,9*S*,10*R*,13*R*,14*S*,17*R*)-14-hydroxy-10,13-dimethyl-3-(3,4,5-trihydroxy-6-methyloxan-2-yl)oxy-1,2,3,6,7,8,9,11,12,15,16,17-dodecahydrocyclopenta[a]phenanthren-17-yl]pyran-2-one (**9**) was reported with highest tendency to inhibit glutathione S-transferase and thioredoxin-glutathione reductase, better than other studied compounds. It was observed that compound **9** have ability to inhibit more than one target as proved in this work. The ADMET properties were investigated and reported in this work.

Authors' contribution

Data availability statement

All data sets were generated or analyzed in the current study.

Funding

Acknowledgments

References

Adeoye, M. D.; Olarinoye, E. F.; Oyebamiji, A. K.; Latona, D. F. Theoretical evaluation of potential anti-alanine dehydrogenase activities of acetamide derivatives. *Biointerface Res. Appl. Chem.* **2022**, *12* (6), 7469–7477. https://doi.org/10.33263/BRIAC126.74697477

Akachukwu, I.; Olubiyi, O. O.; Kosisochukwu, A.; John, M. C.; Justina, N. N. Structure-based study of natural products with anti-schistosoma activity. *Curr. Comput. Aided Drug Des.* **2017**, *13* (2), 91–100. https://doi.org/10.2174/1573409913666170119114859

Allotey, P.; Reidpath, D. D.; Pokhrel, S. Social sciences research in neglected tropical diseases 1: The ongoing neglect in the neglected tropical diseases. *Health Res. Policy Sys.* **2010**, *8*, 32. https://doi.org/10.1186/1478-4505-8-32

Angelucci, F.; Sayed, A. A.; Williams, D. L.; Boumis, G.; Brunori, M.; Dimastrogiovanni, D.; Miele, A. E.; Pauly, F.; Bellelli, A. Inhibition of *Schistosoma mansoni* thioredoxin-glutathione reductase by auranofin. *J. Biol. Chem.* **2009**, *284* (42), 28977–28985. https://doi.org/10.1074/jbc.M109.020701

Colley, D. G.; Bustinduy, A. L.; Secor, W. E.; King, C. H. Human schistosomiasis. *Lancet.* **2014**, *383* (9936), 2253–2264. https://doi.org/10.1016/S0140-6736(13)61949-2

Cunningham, A. B. *An investigation of the herbal medicinal trade in Natal/KwaZulu*. Investigational Report 29; Institute of Natural Resources, 1988.

Engels, D.; Zhou, X.-N. Neglected tropical diseases: An effective global response to local poverty-related disease priorities. *Infect. Dis. Poverty.* **2020**, *9*, 10. https://doi.org/10.1186/s40249-020-0630-9

Eloff, J. N. A Sensitive and quick microplate method to determine the minimal inhibitory concentration of plant extracts for bacteria. *Planta Med.* **1998**, *64* (8) 711–713. https://doi.org/10.1055/s-2006-957563

El-Seedi, H. R.; El-Shabasy, R.; Sakr, H.; Zayed, M.; El-Said, A. M. A.; Helmy, K. M. H.; Gaara, A. H. M.; Turki, Z.; Azeem, M.; Ahmed, A. M.; Boulos, L.; Borg-Karlson, A-K.; Göransson, U. Anti-schistosomiasis triterpene glycoside from the Egyptian medicinal plant *Asparagus stipularis*. *Rev. Bras. Farmacogn.* **2012**, *22* (2), 314–318. https://doi.org/10.1590/S0102-695X2012005000004

Fadladdin, Y. A. J. Evaluation of antischistosomal activities of crude aqueous extracts of *Artemisia annua*, *Nigella sativa*, and *Allium sativum* against *Schistosoma mansoni* in hamsters. *BioMed Res. Inter.* **2022**, *2022*, 5172287. https://doi.org/10.1155/2022/5172287

Hutchings, A. A survey and analysis of traditional medicinal plants as used by the Zulu, Xhosa and Sotho. *Bothalia.* **1989**, *19* (1), a947. https://doi.org/10.4102/abc.v19i1.947

Hutchings, A.; Haxton Scott, A. H.; Lewis, S. G.; Cunningham, A. *Zulu medicinal plants*: An inventory; University of Natal Press, 1996.

Kayuni, S.; Lampiao, F.; Makaula, P.; Juziwelo, L.; Lacourse, E. J.; Reinhard-Rupp, J.; Leutscher, P. D. C.; Stothard, J. R. A systematic review with epidemiological update of male genital schistosomiasis (MGS): A call for integrated case management across the health system in sub-Saharan Africa. *Parasite Epidemiol Control.* **2019**, *4*, e00077. https://doi.org/10.1016/j.parepi.2018.e00077

Klohe, K.; Koudou, B. G.; Fenwick, A.; Fleming, F.; Garba, A.; Gouvras, A.; Harding-Esch, E. M.; Knopp, S.; D'Souza, S.; Utzinger, J.; Vounatsou, P.; Waltz, J.; Zhang, Y.; Rollinson, D. A systematic literature review of schistosomiasis in urban and peri-urban settings. *PLoS Negl. Trop. Dis.* **2021**, *15* (2), e0008995. https://doi.org/10.1371/journal.pntd.0008995

Latona, D. F.; Oyebamiji, A. K.; Mutiu, O. A., Olarinoye, E. F. Evaluation of some benzimidazole derivatives as hepatitis B&C protease inhibitors: Computational study. *Trop. J. Nat. Prod. Res.* **2022a**, *6* (3), 416–421.

Latona, D. F.; Mutiu, O. A.; Adeoye, M. D.; Oyebamiji, A. K.; Akintelu, S. A.; Adedapo, A. S. *In-silico* investigation on chloroquine derivatives: A potential anti-COVID-19 main protease. *Biointerface Res. Appl. Chem.* **2022b**, *12* (6), 8492–8501. https://doi.org/10.33263/BRIAC126.84928501

Lawal, H. A.; Uzairu, A.; Uba, S. QSAR, molecular docking studies, ligand-based design and pharmacokinetic analysis on Maternal Embryonic Leucine Zipper Kinase (MELK) inhibitors as potential anti-triple-negative breast cancer (MDA-MB-231cell line) drug compounds. *Bull. Natl. Res. Centre.* **2021**, *45*, 90. https://doi.org/10.1186/s42269-021-00541-x

Mander, M. *The marketing of indigenous medicinal plants in South Africa: A case study in KwaZulu-Natal*. Investigational Report 164; Institute of Natural Resources, 1997.

McTigue, M. A.; Williams, D. R.; Tainer, J. A. Crystal structures of a schistosomal drug and vaccine target: Glutathione S-transferase from *Schistosoma japonica* and its complex with the leading antischistosomal drug praziquantel. *J. Mol. Biol.* 1995, *246* (1), 21–27. https://doi.org/10.1006/jmbi.1994.0061

Molyneux, D. H. Combating the "other diseases" of MDG 6: Changing the paradigm to achieve equity and poverty reduction? *Trans. R. Soc. Trop. Med. Hyg.* **2008**, *102* (6), 509–519. https://doi.org/10.1016/j.trstmh.2008.02.024

Molyneux, D. H.; Hotez, P. J.; Fenwick, A.; Newman, R. D.; Greenwood, B.; Sachs, J. Neglected tropical diseases and the Global Fund. *Lancet.* **2009**, *373* (9660), 296–297. https://doi.org/10.1016/S0140-6736(09)60089-1

Mtemeli, F. L.; Shoko, R.; Ndlovu, J.; Mugumbate, G. *In silico* study of *Cucurbita maxima* compounds as potential therapeutics against schistosomiasis. *Bioinform. Biol. Insights.* **2022**, *16*, 1–10. https://doi.org/10.1177/11779322221100741

Olasupo, S. B.; Uzairu, A.; Shallangwa, G. A.; Uba, S. Unveiling novel inhibitors of dopamine transporter via in silico drug design, molecular docking, and bioavailability predictions as potential antischizophrenic agents. *Futur. J. Pharm. Sci.* **2021**, *7*, 63. https://doi.org/10.1186/s43094-021-00198-3

Oyeneyin, O. E.; Iwegbulam, C. G.; Ipinloju, N.; Olajide, B. F.; Oyebamiji, A. K. Prediction of the antiproliferative effects of some benzimidazolechalcone derivatives against MCF-7 breast cancer cell lines: QSAR and molecular docking studies. *Org. Commun.* **2022**, *15* (3), 273–277. https://doi.org/10.25135/acg.oc.132.2203.2374

Porto, R.; Mengarda, A. C.; Cajas, R. A.; Salvadori, M. C.; Teixeira, F. S.; Arcanjo, D. D. R.; Siyadatpanah, A.; Pereira, M. L; Wilairatana, P.; Moraes, J. Antiparasitic properties of cardiovascular agents against human intravascular parasite *Schistosoma mansoni. Pharmaceuticals.* **2021**, *14* (7), 686. https://doi.org/10.3390/ph14070686

Reddy, M.; Gill, S. S.; Kalkar, S. R.; Wu, W.; Anderson, P. J.; Rochon, P. A. Oral drug therapy for multiple neglected tropical diseases: A systematic review. *JAMA.* **2007**, *298* (16), 1911–1924. https://doi.org/10.1001/jama.298.16.1911

Saranya, M.; Ayyappan, S.; Nithya, R.; Sangeetha, R. K.; Gokila, A. Molecular structure, NBO and HOMO-LUMO analysis of quercetin on single layer graphene by density functional theory. *Dig. J. Nanomater. Biostructures.* **2018**, *13* (1), 97–105.

Sparg, S. G.; van Staden, J.; Jäger, A. K. Pharmacological and phytochemical screening of two Hyacinthaceae species: *Scilla natalensis* and *Ledebouria ovatifolia. J. Ethnopharmacol.* **2002**, *80* (1), 95–101. https://doi.org/10.1016/S0378-8741(02)00007-7

Ugbe, F. A.; Shallangwa, G. A.; Uzairu, A.; Abdulkadir, I. Theoretical modeling and design of some pyrazolopyrimidine derivatives as *Wolbachia inhibitors*, targeting lymphatic filariasis and onchocerciasis. *In Silico Pharmacol.* **2022**, *10*, 8. https://doi.org/10.1007/s40203-022-00123-3

Wang, X.; Dong, H.; Qin, Q. QSAR models on aminopyrazole substituted resorcylate compounds as Hsp90 inhibitors. *J. Comput. Sci. Eng.* **2020**, *48*, 1146–1156.

World Health Organization (WHO). *Schistosomiasis*. Fact Sheet No 115; WHO, 2020. http://www.who.int/mediacentre/factsheets/fs115/en/. (accessed 2020-Jan-20)

World Health Organization (WHO). *Control of neglected tropical diseases*; WHO, 2022. http://www.who.int/teams/control-of-neglected-tropical-diseases/overview. (accessed 2020-Jan-20)

Supplementary Material 1

Figure S1. Predicted orbital energy for compound 1.

Figure S2. Predicted orbital energy for compound 2.

Figure S3. Predicted orbital energy for compound 3.

Figure S4. Predicted orbital energy for compound 4.

Figure S5. Predicted orbital energy for compound 5.

Figure S6. Predicted orbital energy for compound 6,

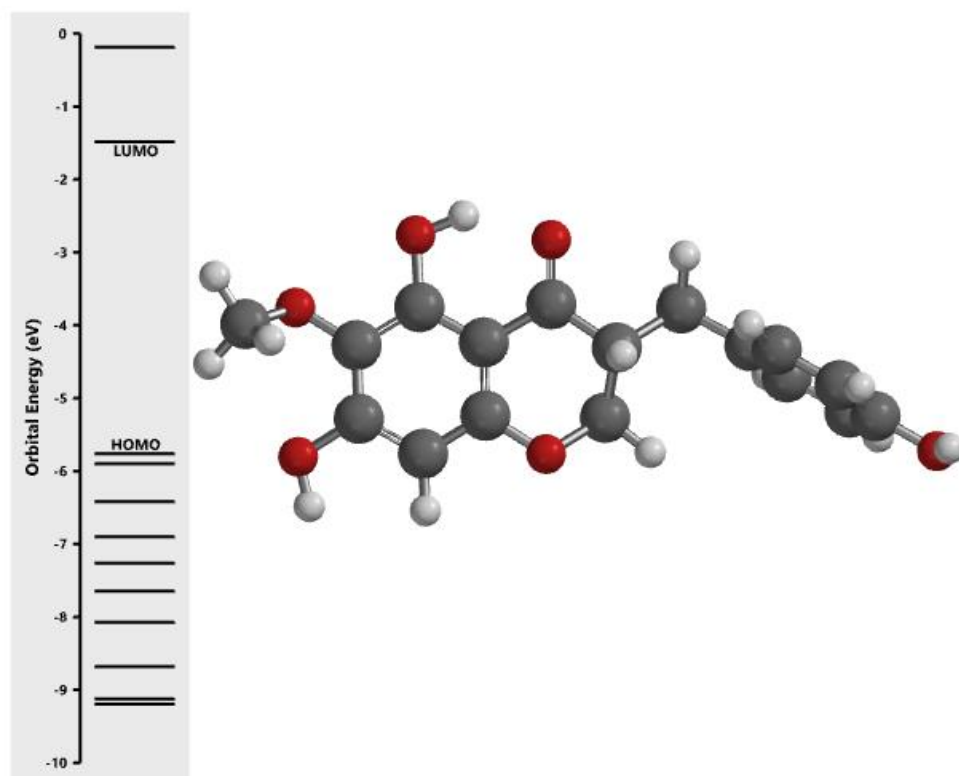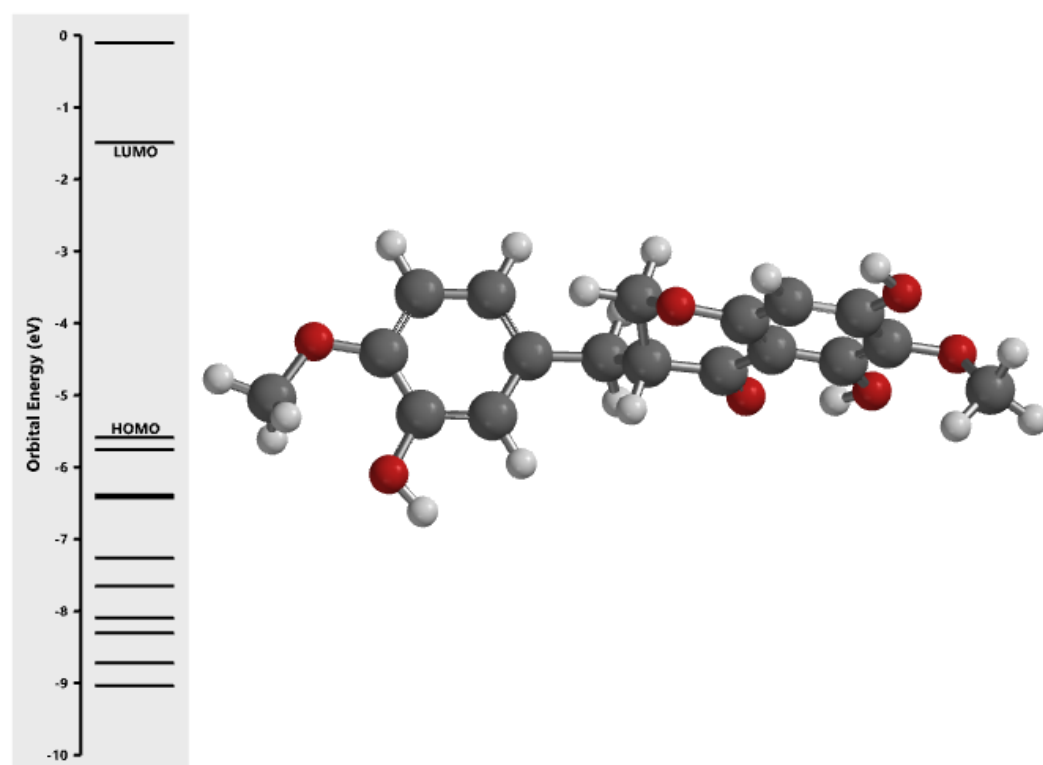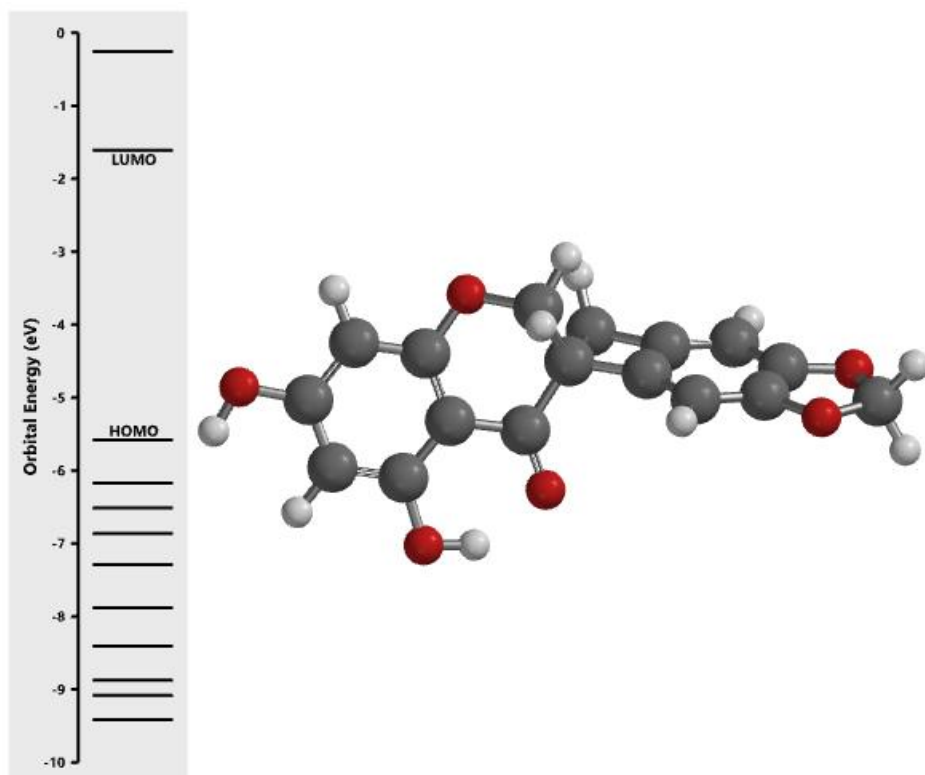**Figure S7.** Predicted orbital energy for compound 7.
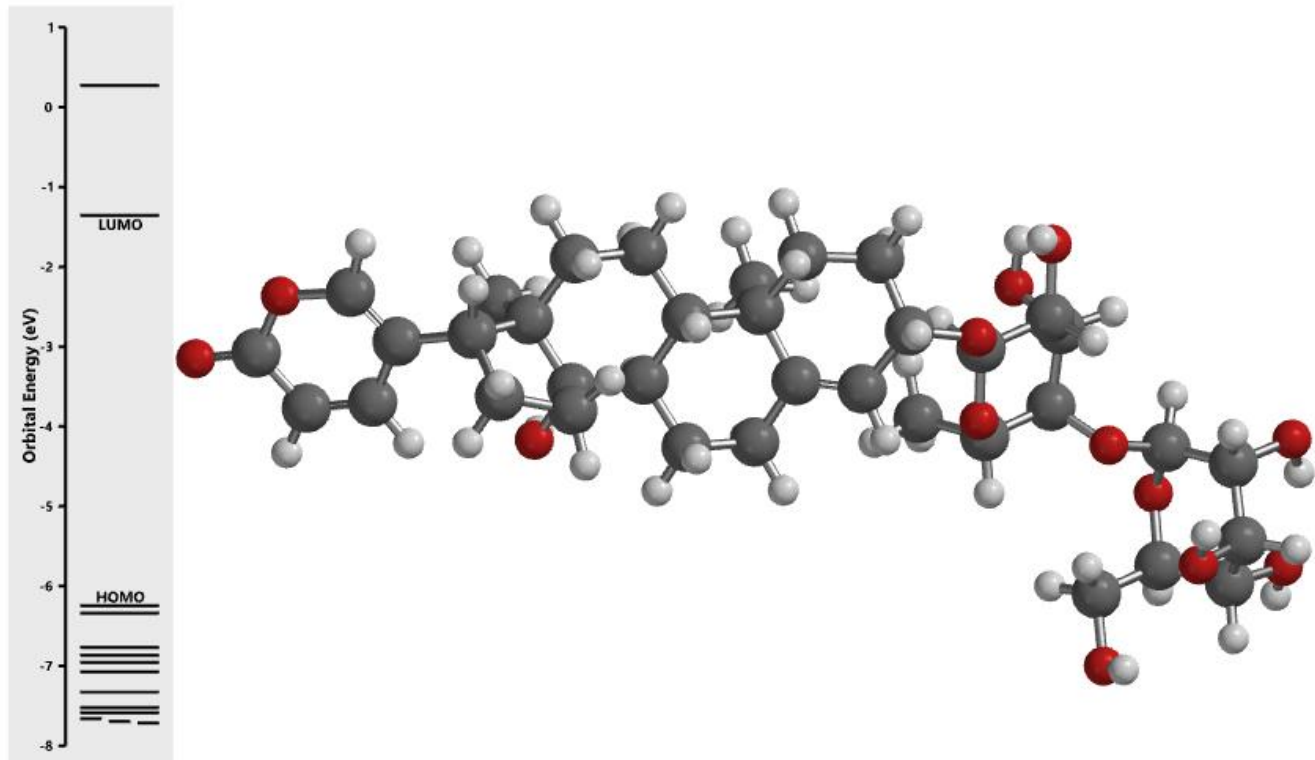
Figure S8. Predicted orbital energy for compound 8.
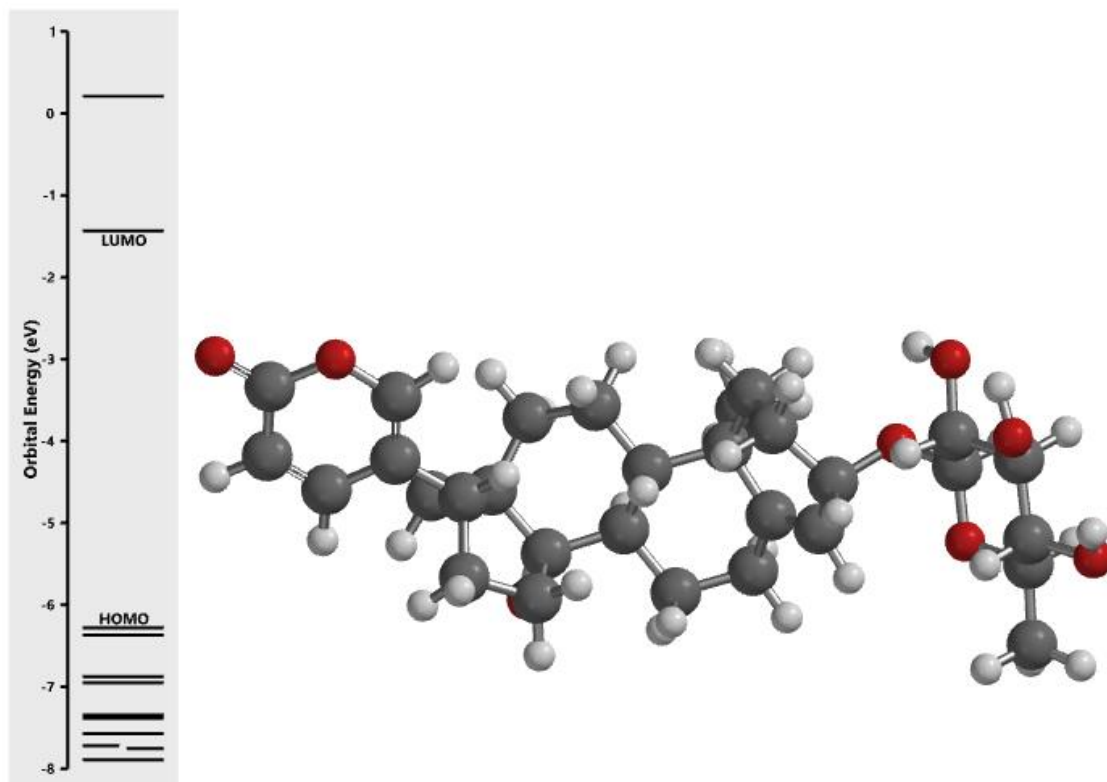
Figure S9. Predicted orbital energy for compound 9.
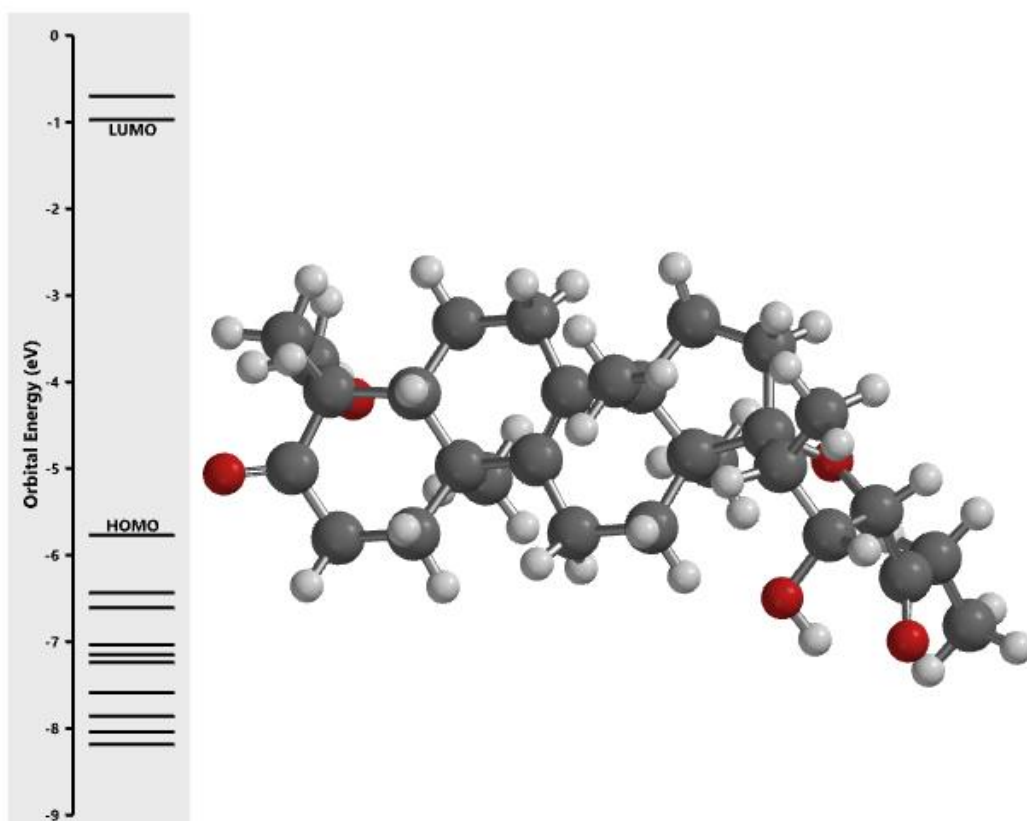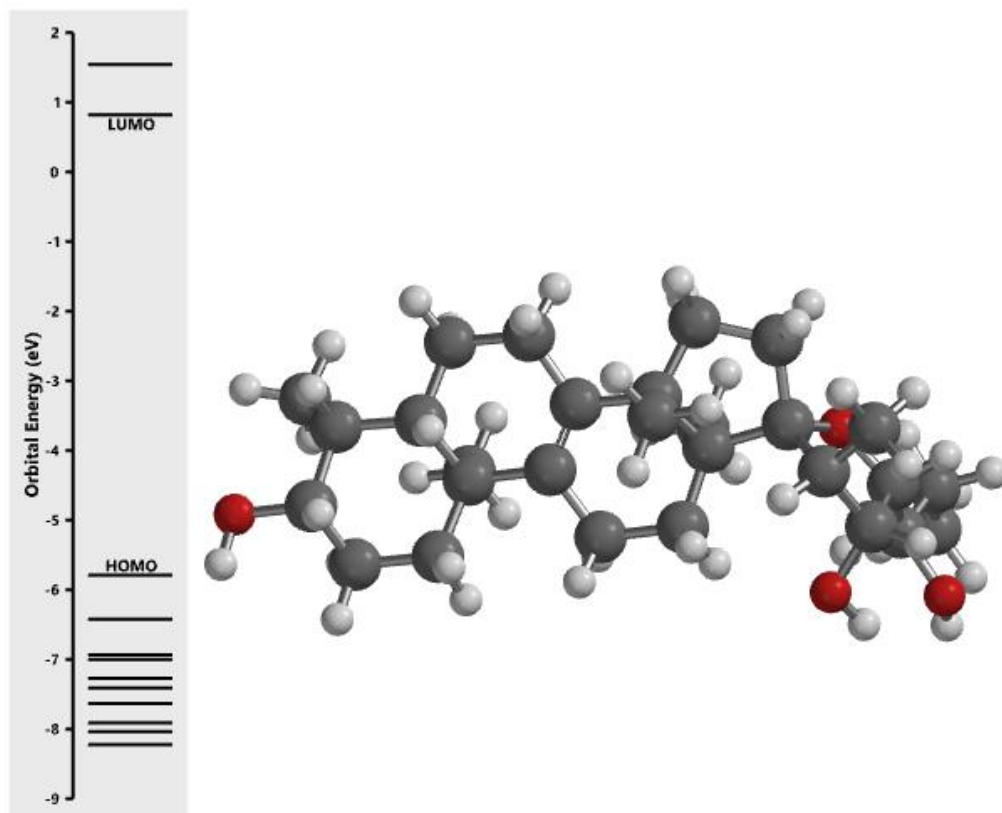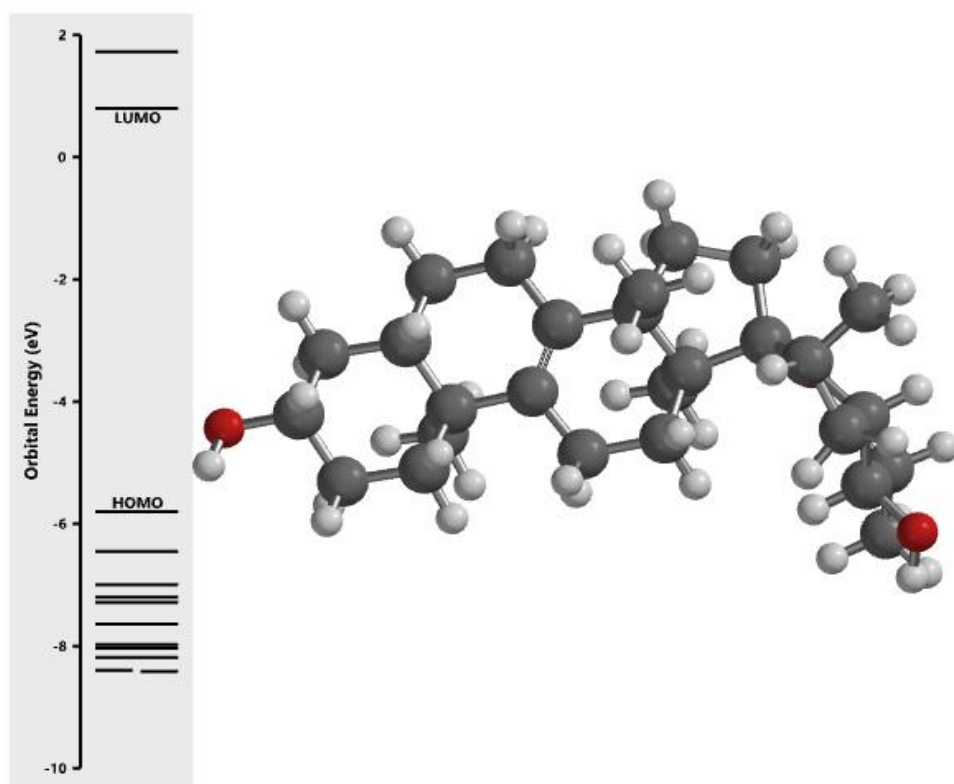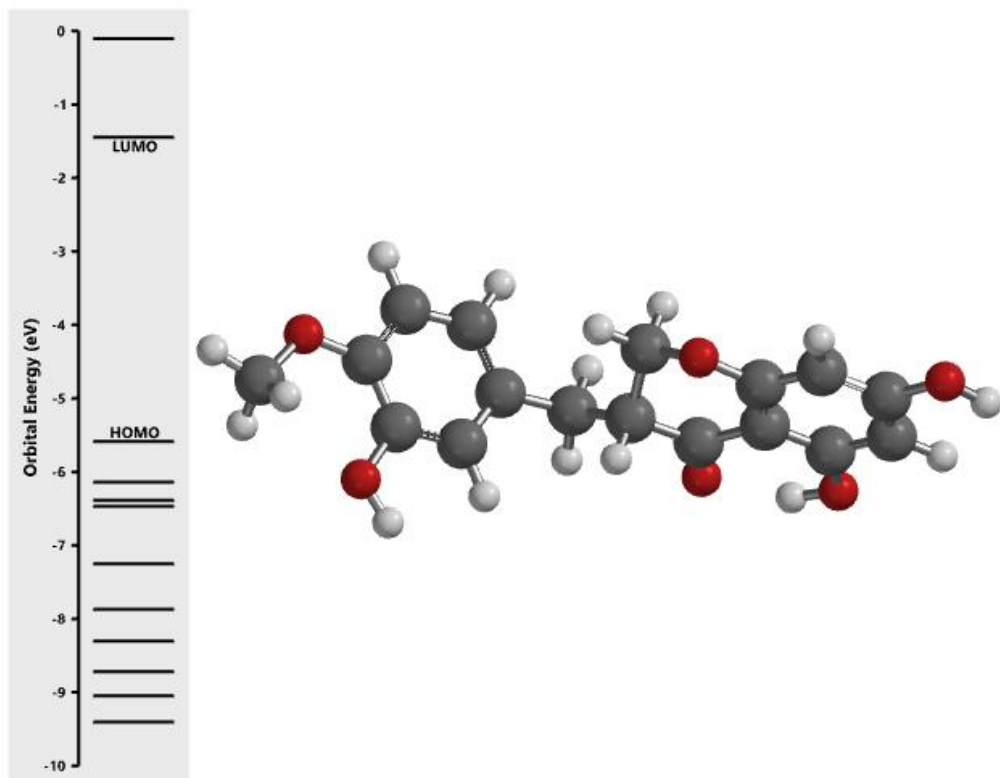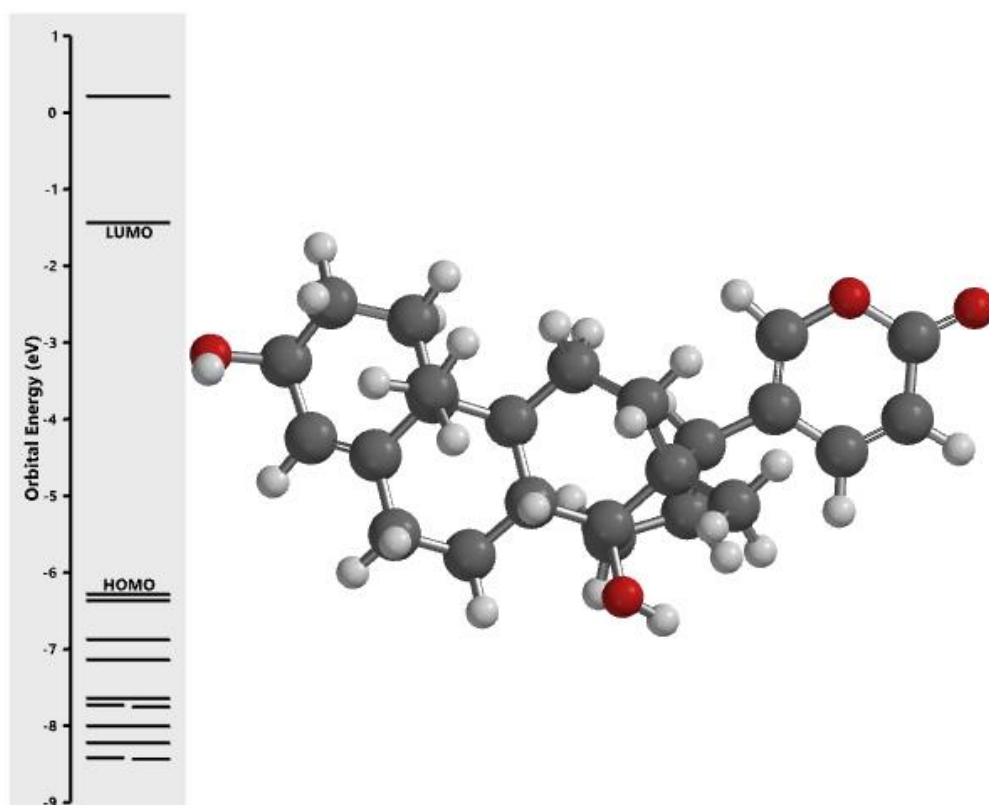

Figure S10. Predicted orbital energy for compound 10.

Supplementary Material 2

Compound 9

Table S1. Physicochemical property.

Property	Value	Comment
Molecular Weight	530.29	Contain hydrogen atoms. Optimal:100~600
Volume	535.873	Van der Waals volume
Density	0.99	Density = MW / volume
nHA	8	Number of hydrogen bond acceptors. Optimal:0~12
nHD	4	Number of hydrogen bond donors. Optimal:0~7
nRot	3	Number of rotatable bonds. Optimal:0~11
nRing	6	Number of rings. Optimal:0~6
MaxRing	17	Number of atoms in the biggest ring. Optimal:0~18
nHet	8	Number of heteroatoms. Optimal:1~15
fChar	0	Formal charge. Optimal: –4 ~4
nRig	33	Number of rigid bonds. Optimal:0~30
Flexibility	0.091	Flexibility = nRot /nRig
Stereo Centers	12	Optimal: ≤ 2
TPSA	129.59	Topological Polar Surface Area. Optimal:0~140
logS	–4.093	Log of the aqueous solubility. Optimal: –4~0.5 log mol L^{-1}
logP	2.698	Log of the octanol/water partition coefficient. Optimal: 0~3
logD	2.071	LogP at physiological pH 7.4. Optimal: 1~3

Table 2. Medicinal Chemistry.

Property	Value	Decision	Comment
QED	0.439	●	A measure of drug-likeness based on the concept of desirability. Attractive: > 0.67; unattractive: 0.49~0.67; too complex: < 0.34.
SAscore	5.052	●	Synthetic accessibility score is designed to estimate ease of synthesis of drug-like molecules. SAscore $\geq$ 6, difficult to synthesize; SAscore < 6, easy to synthesize.
Fsp3	0.767	●	The number of sp3 hybridized carbons / total carbon count, correlating with melting point and solubility. Fsp^3 $\geq$ 0.42 is considered a suitable value.
MCE-18	146.434	●	MCE-18 stands for medicinal chemistry evolution. MCE-18 $\geq$ 45 is considered a suitable value.
NPscore	2.731	-	Natural product-likeness score. This score is typically in the range from –5 to 5. The higher the score is, the higher the probability is that the molecule is a NP.
Lipinski Rule	Accepted	●	MW $\leq$ 500; logP $\leq$ 5; Hacc $\leq$ 10; Hdon $\leq$ 5 If two properties are out of range, a poor absorption or permeability is possible, one is acceptable.
Pfizer Rule	Accepted	●	logP > 3; TPSA < 75 Compounds with a high log P (>3) and low TPSA (<75) are likely to be toxic.
GSK Rule	Rejected	●	MW $\leq$ 400; logP $\leq$ 4 Compounds satisfying the GSK rule may have a more favorable ADMET profile
Golden Triangle	Rejected	●	200 $\leq$ MW $\leq$ 50; -2 $\leq$ logD $\leq$ 5 Compounds satisfying the Golden Triangle rule may have a more favorable ADMET profile.
PAINS	0 alert	-	Pan Assay Interference Compounds, frequent hitters, Alpha-screen artifacts and reactive compound.
ALARM NMR	1 alert	-	Thiol reactive compounds.
BMS	0 alert	-	Undesirable, reactive compounds.
Chelator Rule	0 alert	-	Chelating compounds.

Table S3. Absorption.

Property	Value	Decision	Comment
Caco-2 Permeability	–5.037	●	Optimal: higher than –5.15 Log unit.
MDCK Permeability	2.3×10^{05}	●	Low permeability: $< 2 \times 10^{-6}$ cm s^{-1} Medium permeability: 2–20×10^{-6} cm s^{-1} High passive permeability: $> 20 \times 10^{-6}$ cm s^{-1}
Pgp-inhibitor	0.395	●	Category 1: Inhibitor; Category 0: Noninhibitor. The output value is the probability of being Pgp-inhibitor.
Pgp-substrate	0.998	●	Category 1: substrate; Category 0: Nonsubstrate. The output value is the probability of being Pgp-substrate.
HIA	0.88	●	Human intestinal absorption Category 1: HIA+(HIA < 30%); Category 0: HIA–(HIA < 30%); The output value is the probability of being HIA+
F 20%	0.985	●	20% Bioavailability Category 1: F + (bioavailability < 20%). 20% Category 0: F – (bioavailability ≥ 20%); The output 20% value is the probability of being F+ 20%
F 30%	0.99	●	30% Bioavailability Category 1: F + (bioavailability < 30%). 30% Category 0: F – (bioavailability ≥ 30%); The output 30% value is the probability of being F+ 30%

Table S4. Distribution.

Property	Value	Decision	Comment
PPB	86.87%	●	Plasma protein binding Optimal: < 90%. Drugs with high protein-bound may have a low therapeutic index.
VD	1.468	●	Volume distribution Optimal: 0.04–20 L kg^{-1}
BBB penetration	0.085	●	Blood-brain barrier penetration Category 1: BBB+; Category 0: BBB-; The output value is the probability of being BBB+
FU	6.943%	●	The fraction unbound in plasms Low: < 5%; Middle: 5~20%; High: > 20%

Table S5. Metabolism.

Property	Value	Comment
CYP1A2 inhibitor	0.019	Category 1: Inhibitor; Category 0: Noninhibitor. The output value is the probability of being inhibitor.
CYP1A2 substrate	0.883	Category 1: Substrate; Category 0: Nonsubstrate. The output value is the probability of being substrate.
CYP2C19 inhibitor	0.044	Category 1: Inhibitor; Category 0: Noninhibitor. The output value is the probability of being inhibitor.
CYP2C19 substrate	0.615	Category 1: Substrate; Category 0: Nonsubstrate. The output value is the probability of being substrate.
CYP2C9 inhibitor	0.123	Category 1: Inhibitor; Category 0: Noninhibitor. The output value is the probability of being inhibitor.
CYP2C9 substrate	0.072	Category 1: Substrate; Category 0: Nonsubstrate. The output value is the probability of being substrate.
CYP2D6 inhibitor	0.024	Category 1: Inhibitor; Category 0: Noninhibitor. The output value is the probability of being inhibitor.
CYP2D6 substrate	0.37	Category 1: Substrate; Category 0: Nonsubstrate. The output value is the probability of being substrate.
CYP3A4 inhibitor	0.429	Category 1: Inhibitor; Category 0: Noninhibitor; The output value is the probability of being inhibitor.
CYP3A4 substrate	0.284	Category 1: Substrate; Category 0: Nonsubstrate. The output value is the probability of being substrate.

Table S6. Excretion.

Property	Value	Decision	Comment
CL	3.333	●	Clearance High: > 15 mL min^{-1} kg^{-1}; Moderate: 5–15 mL min^{-1} kg^{-1}. Low: < 5 mL min^{-1} kg^{-1}.
T$_{1/2}$	0.306	-	Category 1: long half-life; Category 0: short half-life. Long half-life: > 3 h; Short half-life: < 3 h. The output value is the probability of having long half-life.

Table S7. Toxicity.

Property	Value	Decision	Comment
hERG blockers	0.436	●	Category 1: active; Category 0: inactive. The output value is the probability of being active.
H-HT	0.236	●	Human hepatotoxicity Category 1: H-HT positive(+); Category 0: H-HT negative(–). The output value is the probability of being toxic.
DILI	0.153	●	Drug induced liver injury. Category 1: drugs with a high risk of DILI; Category 0: drugs with no risk of DILI. The output value is the probability of being toxic.
AMES toxicity	0.066	●	Category 1: AMES positive(+); Category 0: AMES negative(–). The output value is the probability of being toxic.
Rat oral acute toxicity	0.846	●	Category 0: low toxicity; Category 1: high toxicity. The output value is the probability of being highly toxic.
FDAMDD	0.93	●	Maximum Recommended Daily Dose. Category 1: FDAMDD (+); Category 0: FDAMDD (–). The output value is the probability of being positive.
Skin sensitization	0.131	●	Category 1: Sensitizer; Category 0: Nonsensitizer. The output value is the probability of being sensitizer.
Carcinogen city	0.768	●	Category 1: carcinogens; Category 0: noncarcinogens. The output value is the probability of being toxic.
Eye corrosion	0.003	●	Category 1: corrosives; Category 0: noncorrosives. The output value is the probability of being corrosives.
Eye irritation	0.011	●	Category 1: irritants; Category 0: nonirritants. The output value is the probability of being irritants.
Respiratory toxicity	0.957	●	Category 1: respiratory toxicants; Category 0: respiratory nontoxicants. The output value is the probability of being toxic.

Table S8. Environmental toxicity.

Property	Value	Comment
Bioconcentration Factors	1.055	Bioconcentration factors are used for considering secondary poisoning potential and assessing risks to human health via the food chain. The unit is $-\log10[(\text{mg L}^{-1})/(1000 \times \text{MW})]$
IGC 50	3.631	Tetrahymena pyriformis 50% growth inhibition concentration The unit is $-\log10[(\text{mg L}^{-1})/(1000 \times \text{MW})]$
LC FM 50	6.124	96-h fathead minnow 50% lethal concentration The unit is $-\log10[(\text{mg L}^{-1})/(1000 \times \text{MW})]$
LC DM 50	6.207	48-h daphnia magna 50% lethal concentration The unit is $-\log10[(\text{mg L}^{-1})/(1000 \times \text{MW})]$

Table S9. Tox21 pathway.

Property	Value	Decision	Comment
NR-AR	0.886	●	Androgen receptor Category 1: active; Category 0: inactive. The output value is the probability of being active.
NR-AR-LBD	0.975	●	Androgen receptor ligand-binding domain. Category 1: active; Category 0: inactive. The output value is the probability of being active.
NR-AhR	0.003	●	Aryl hydrocarbon receptor Category 1: active; Category 0: inactive. The output value is the probability of being active.
NR-aromatase	0.852	●	Category 1: active; Category 0: inactive. The output value is the probability of being active.
NR-ER	0.932	●	Estrogen receptor Category 1: active; Category 0: inactive. The output value is the probability of being active.
NR-ER-LBD	0.131	●	Estrogen receptor ligand-binding domain Category 1: active; Category 0: inactive. The output value is the probability of being active.
NR-PPAR- gamma	0.916	●	Peroxisome proliferator-activated receptor gamma Category 1: active; Category 0: inactive. The output value is the probability of being active.
SR-ARE	0.725	●	Antioxidant response element Category 1: active; Category 0: inactives; The output value is the probability of being active.
SR-ATAD5	0.701	●	ATPase family AAA domain-containing protein 5 Category 1: active; Category 0: inactive. The output value is the probability of being active.
SR-HSE	0.095	●	Heat shock factor response element Category 1: active; Category 0: inactive. The output value is the probability of being active.
SR-MMP	0.927	●	Mitochondrial membrane potential Category 1: active; Category 0: inactive. The output value is the probability of being active.
SR-p53	0.942	●	Category 1: active; Category 0: inactive. The output value is the probability of being active.

Table S10. Toxicophore rules.

Property	Value	Comment
Acute toxicity rule	0 alerts	20 substructures acute toxicity during oral administration
Genotoxic carcinogenicity rule	0 alerts	117 substructures carcinogenicity or mutagenicity
Nongenotoxic carcinogenicity rule	0 alerts	23 substructures carcinogenicity through nongenotoxic mechanisms
Skin sensitization rule	1 alert	155 substructures skin irritation
Aquatic toxicity rule	3 alerts	99 substructures toxicity to liquid(water)
Nonbiodegradable rule	1 alert	19 substructures non-biodegradable
SureChEMBL rule	0 alerts	164 substructures MedChem unfriendly status

Supplementary Material 3

Praziquantel

Table 1. Physicochemical property.

Property	Value	Comment
Molecular Weight	312.18	Contain hydrogen atoms. Optimal:100~600
Volume	329.346	Van der Waals volume
Density	0.948	Density = MW / volume
nHA	4	Number of hydrogen bond acceptors. Optimal:0~12
nHD	0	Number of hydrogen bond donors. Optimal:0~7
nRot	2	Number of rotatable bonds. Optimal:0~11
nRing	4	Number of rings. Optimal:0~6
MaxRing	14	Number of atoms in the biggest ring. Optimal:0~18
nHet	4	Number of heteroatoms. Optimal:1~15
fChar	0	Formal charge. Optimal: -4 ~4
nRig	24	Number of rigid bonds. Optimal:0~30
Flexibility	0.083	Flexibility = nRot /nRig
Stereo Centers	1	Optimal: ≤ 2
TPSA	40.62	Topological polar surface area. Optimal:0~140
logS	-2.484	Log of the aqueous solubility. Optimal: -4~0.5 log mol/L
logP	2.758	Log of the octanol/water partition coefficient. Optimal: 0~3
logD	2.492	logP at physiological pH 7.4. Optimal: 1~3

Table 2. Medicinal Chemistry.

Property	Value	Decision	Comment
QED	0.799	●	A measure of drug-likeness based on the concept of desirability. Attractive: > 0.67; Unattractive: 0.49~0.67; Too complex: < 0.34.
SAscore	2.709	●	Synthetic accessibility score is designed to estimate ease of synthesis of drug-like molecules. SAscore $\geq$ 6, difficult to synthesize; SAscore < 6, easy to synthesize.
Fsp3	0.579	●	The number of sp3 hybridized carbons / total carbon count, correlating with melting point and solubility. $Fsp^3 \geq 0.42$ is considered a suitable value.
MCE-18	74.667	●	MCE-18 stands for medicinal chemistry evolution. MCE-18 $\geq$ 45 is considered a suitable value.
NPscore	-0.813	-	Natural product-likeness score. This score is typically in the range from –5 to 5. The higher the score is, the higher the probability is that the molecule is a NP.
Lipinski Rule	Accepted	●	MW $\leq$ 500; logP $\leq$ 5; Hacc $\leq$ 10; Hdon $\leq$ 5. If two properties are out of range, a poor absorption or permeability is possible, one is acceptable.
Pfizer Rule	Accepted	●	logP > 3; TPSA < 75. Compounds with a high log P (>3) and low TPSA (<75) are likely to be toxic.
GSK Rule	Accepted	●	MW $\leq$ 400; logP $\leq$ 4 Compounds satisfying the GSK rule may have a more favorable ADMET profile.
Golden Triangle	Accepted	●	200 $\leq$ MW $\leq$ 50; –2 $\leq$ logD $\leq$ 5. Compounds satisfying the Golden Triangle rule may have a more favorable ADMET profile.
PAINS	0 alerts	-	Pan assay interference compounds, frequent hitters, Alpha-screen artifacts and reactive compound.
ALARM NMR	0 alerts	-	Thiol reactive compounds.
BMS	0 alerts	-	Undesirable, reactive compounds.
Chelator Rule	0 alerts	-	Chelating compounds.

Table S3. Absorption.

Property	Value	Decision	Comment
Caco-2 permeability	–4.923	●	Optimal: higher than –5.15 Log unit
MDCK Permeability	2.6x10⁻⁰⁵	●	Low permeability: $< 2 \times 10^{-6}$ cm s^{-1} Medium permeability: $2\text{–}20 \times 10^{-6}$ cm s^{-1} High passive permeability: $> 20 \times 10^{-6}$ cm s^{-1}
Pgp-inhibitor	0.226	●	Category 1: Inhibitor; Category 0: Noninhibitor. The output value is the probability of being Pgp-inhibitor.
Pgp-substrate	0.105	●	Category 1: substrate; Category 0: Nonsubstrate. The output value is the probability of being Pgp-substrate.
HIA	0.006	●	Human intestinal absorption Category 1: HIA+(HIA < 30%); Category 0: HIA-(HIA < 30%); The output value is the probability of being HIA+.
F 20%	0.991	●	20% Bioavailability Category 1: F + (bioavailability < 20%); 20% Category 0: F – (bioavailability ≥ 20%); The output 20% value is the probability of being F + 20%
F 30%	0.995	●	30% Bioavailability Category 1: F + (bioavailability < 30%). 30% Category 0: F – (bioavailability ≥ 30%); The output 30% value is the probability of being F + 30%

Table S4. Distribution.

Property	Value	Decision	Comment
PPB	93.68%	●	Plasma protein binding Optimal: < 90%. Drugs with high protein-bound may have a low therapeutic index.
VD	0.662	●	Volume distribution Optimal: 0.04–20 L kg⁻¹.
BBB Penetration	0.997	●	Blood-Brain Barrier Penetration Category 1: BBB+; Category 0: BBB–; The output value is the probability of being BBB+
FU	7.573%	●	The fraction unbound in plasms Low: < 5%; Middle: 5~20%; High: > 20%

Table S5. Metabolism.

Property	Value	Comment
CYP1A2 inhibitor	0.051	Category 1: Inhibitor; Category 0: Noninhibitor. The output value is the probability of being inhibitor.
CYP1A2 substrate	0.447	Category 1: Substrate; Category 0: Nonsubstrate. The output value is the probability of being substrate.
CYP2C19 inhibitor	0.887	Category 1: Inhibitor; Category 0: Non- inhibitor. The output value is the probability of being inhibitor.
CYP2C19 substrate	0.801	Category 1: Substrate; Category 0: Nonsubstrate. The output value is the probability of being substrate.
CYP2C9 inhibitor	0.796	Category 1: Inhibitor; Category 0: Noninhibitor. The output value is the probability of being inhibitor.
CYP2C9 substrate	0.923	Category 1: Substrate; Category 0: Nonsubstrate. The output value is the probability of being substrate.
CYP2D6 inhibitor	0.031	Category 1: Inhibitor; Category 0: Non- inhibitor. The output value is the probability of being inhibitor.
CYP2D6 substrate	0.64	Category 1: Substrate; Category 0: Nonsubstrate. The output value is the probability of being substrate.
CYP3A4 inhibitor	0.771	Category 1: Inhibitor; Category 0: Non- inhibitor. The output value is the probability of being inhibitor.
CYP3A4 substrate	0.678	Category 1: Substrate; Category 0: Nonsubstrate. The output value is the probability of being substrate.

Table S6. Excretion.

Property	Value	Decision	Comment
CL	2.683	●	Clearance High: >15 mL min^{-1} kg^{-1}; Moderate: 5–15 mL min^{-1} kg^{-1}; Low: < 5 mL min^{-1} kg^{-1}
T$_{1/2}$	0.43	-	Category 1: long half-life; Category 0: short half-life. Long half-life: > 3 h; Short half-life: < 3 h. The output value is the probability of having long half-life.

Table S7. Toxicity.

Property	Value	Decision	Comment
hERG Blockers	0.106	●	Category 1: active; Category 0: inactive. The output value is the probability of being active.
H-HT	0.922	●	Human hepatotoxicity Category 1: H-HT positive(+); Category 0: H-HT negative (–). The output value is the probability of being toxic.
DILI	0.166	●	Drug induced liver injury. Category 1: drugs with a high risk of DILI; Category 0: drugs with no risk of DILI. The output value is the probability of being toxic.
AMES Toxicity	0.007	●	Category 1: AMES positive(+); Category 0: AMES negative(-). The output value is the probability of being toxic.
Rat Oral Acute Toxicity	0.515	●	Category 0: low toxicity; Category 1: high toxicity. The output value is the probability of being highly toxic.
FDAMDD	0.929	●	Maximum recommended daily dose Category 1: FDAMDD (+); Category 0: FDAMDD (–). The output value is the probability of being positive.
Skin sensitization	0.713	●	Category 1: sensitizer; Category 0: nonsensitizer. The output value is the probability of being sensitizer.
Carcinogen city	0.187	●	Category 1: carcinogens; Category 0: noncarcinogens. The output value is the probability of being toxic.
Eye corrosion	0.003	●	Category 1: corrosive; Category 0: noncorrosive. The output value is the probability of being corrosives.
Eye irritation	0.013	●	Category 1: irritant; Category 0: nonirritant. The output value is the probability of being irritants.
Respiratory toxicity	0.056	●	Category 1: respiratory toxicants; Category 0: respiratory nontoxicant. The output value is the probability of being toxic.

Table S8. Environmental toxicity.

Property	Value	Comment
Bioconcentration Factors	0.523	Bioconcentration factors are used for considering secondary poisoning potential and assessing risks to human health via the food chain. The unit is $-\log10[(mg\ L^{-1})/(1000 \times MW)]$
IGC 50	3.145	Tetrahymena pyriformis 50% growth inhibition concentration The unit is $-\log10[(mg\ L^{-1})/(1000 \times MW)]$
LC FM 50	3.915	96-hour fathead minnow 50% lethal concentration The unit is $-\log10[(mg\ L^{-1})/(1000 \times MW)]$
LC DM 50	4.834	48-hour daphnia magna 50% lethal concentration The unit is $-\log10[(mg\ L^{-1})/(1000 \times MW)]$

Table S9. Tox21 pathway.

Property	Value	Decision	Comment
NR-AR	0.773	● (red)	Androgen receptor Category 1: active; Category 0: inactive. The output value is the probability of being active.
NR-AR-LBD	0.047	● (green)	Androgen receptor ligand-binding domain Category 1: active; Category 0: inactive. The output value is the probability of being active.
NR-AhR	0.237	● (green)	Aryl hydrocarbon receptor Category 1: active; Category 0: inactive. The output value is the probability of being active.
NR-aromatase	0.055	● (green)	Category 1: active; Category 0: inactive. The output value is the probability of being active.
NR-ER	0.348	● (orange)	Estrogen receptor Category 1: active; Category 0: inactive. The output value is the probability of being active.
NR-ER-LBD	0.004	● (green)	Estrogen receptor ligand-binding domain Category 1: active; Category 0: inactive. The output value is the probability of being active.
NR-PPAR-gamma	0.145	● (green)	Peroxisome proliferator-activated receptor gamma Category 1: active; Category 0: inactive. The output value is the probability of being active.
SR-ARE	0.462	● (orange)	Antioxidant response element Category 1: active; Category 0: inactive. The output value is the probability of being active.
SR-ATAD5	0.006	● (green)	ATPase family AAA domain-containing protein 5. Category 1: active; Category 0: inactive. The output value is the probability of being active.
SR-HSE	0.034	● (green)	Heat shock factor response element Category 1: actives; Category 0: inactives; The output value is the probability of being active.
SR-MMP	0.124	● (green)	Mitochondrial membrane potential Category 1: actives; Category 0: inactives; The output value is the probability of being active.
SR-p53	0.028	● (green)	Category 1: actives; Category 0: inactives; The output value is the probability of being active.

Table S10. Toxicophore rules.

Property	Value	Comment
Acute toxicity rule	0 alerts	20 substructures acute toxicity during oral administration
Genotoxic carcinogenicity rule	0 alerts	117 substructures carcinogenicity or mutagenicity
Nongenotoxic carcinogenicity rule	0 alerts	23 substructures carcinogenicity through nongenotoxic mechanisms
Skin sensitization rule	1 alert	155 substructures skin irritation
Aquatic toxicity rule	0 alerts	99 substructures toxicity to liquid (water)
Nonbiodegradable rule	0 alerts	19 substructures nonbiodegradable
SureChEMBL rule	0 alerts	164 substructures MedChem unfriendly status